Bioconjugate Chemistry

Article

pubs.acs.org/bc



# *cla*MP Tag: A Versatile Inline Metal-Binding Platform Based on the Metal Abstraction Peptide

Brittney J. Mills,[†] Qingxin Mu,[§] Mary E. Krause,[§] and Jennifer S. Laurence*[,§]

[†]Department of Chemistry, The University of Kansas, Lawrence, Kansas 66045, United States

[§]Department of Pharmaceutical Chemistry, The University of Kansas, Lawrence, Kansas 66047, United States

**ABSTRACT:** Molecularly targeted research and diagnostic tools are essential to advancing understanding and detection of many diseases. Metals often impart the desired functionality to these tools, and conjugation of high-affinity chelators to proteins is carried out to enable targeted delivery of the metal. This approach has been much more effective with large lanthanide series metals than smaller transition metals. Because chemical conjugation requires additional processing and purification steps and yields a heterogeneous mixture of products, inline incorporation of a peptide tag capable of metal binding is a highly preferable alternative. Development of a transition metal binding tag would provide opportunity to greatly expand metal-based analyses. The metal abstraction peptide (MAP) sequence was genetically engineered into recombinant protein to generate the *cla*MP Tag. The effects of this tag on recombinant epidermal growth factor (EGF) protein expression, disulfide bond formation, tertiary structural integrity, and transition metal incorporation using nickel were examined to confirm the viability of utilizing the MAP sequence to generate linker-less metal conjugates.

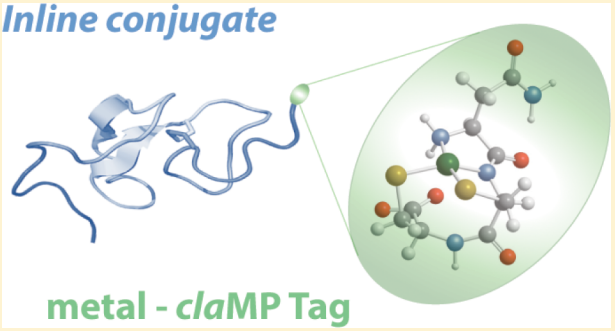


## INTRODUCTION

Metals are extremely useful tools for clinical and biotechnology applications. Metal-based diagnostic imaging is common and its applications include molecular targeting to identify specific cell populations.[1,2] Addition of metal-binding modalities to proteins has been accomplished primarily through chemical conjugation.[3] Attaching a chelating agent requires use of a secondary chemistry, which leads to a heterogeneous mixture of products and requires optimization of the reaction conditions and additional purification steps to recover the desired product.[3−6] These reactions are inefficient, utilizing significant excesses of materials, and significantly increase the time needed to obtain a purified final product.

Incorporation of a peptide-based metal-binding tag into a protein during expression to generate an inline carrier eliminates the need for subsequent modification, greatly simplifying the production of metal-based conjugates. Inline lanthanide-binding peptide tags (LBTs) have been developed for binding to larger metal ions, such as gadolinium, demonstrating the validity of this principle.[7−10] They are large (∼14−20 amino acids) because they must contain six residues positioned appropriately to enable binding to lanthanide ions (Tb(III), Gd(III), Dy(III))[7] using eight oxygen ligands. The presence of a ninth exchangeable water ligand allows for the application of LBTs as MRI contrast agents.[7,9] In the laboratory, LBTs are used in luminescence energy transfer studies[10] and for luminescence-based detection on gels.[7] In addition, paramagnetic lanthanide ions are incorporated into LBTs for use as magnetic-field relaxation and alignment agents in NMR spectroscopy for evaluating protein structure.[8,11] Lanthanide binding tags have found large utility as imaging agents; however, lanthanides are reported to induce significant adverse effects in some patient populations,[12−14] indicating additional approaches are needed. Utilization of more biologically compatible transition metals is desirable, but the inability to achieve appropriate binding to these smaller metal ions by traditional chelators has hindered their use in the clinic.[15−17] Nature typically accomplishes tight binding and control of transition metals using sophisticated protein scaffolds in which the metal is well protected from facile exchange. These highly structured environments are absent in small peptides, which typically results in weaker binding and easier release of the metal to high affinity chelators, such as EDTA. Thus, a tag capable of sequestering smaller metals would enable new tools and provide opportunity to expand therapeutic and diagnostic applications.

Our lab discovered the metal abstraction peptide (MAP) and its novel chemistry that binds transition metals and develops a uniquely structured product with compatible properties for use in clinical applications.[18] The structure is extremely stable under basic conditions, resisting metal release and loss to high affinity chelators in competition experiments, but undergoes rearrangement upon acidification, permitting rapid exchange or release of the metal (manuscript in preparation). MAP is

**Received:** March 17, 2014
**Revised:** April 15, 2014
**Published:** May 7, 2014

   dx.doi.org/10.1021/bc500115h | *Bioconjugate Chem.* 2014, 25, 1103−1111

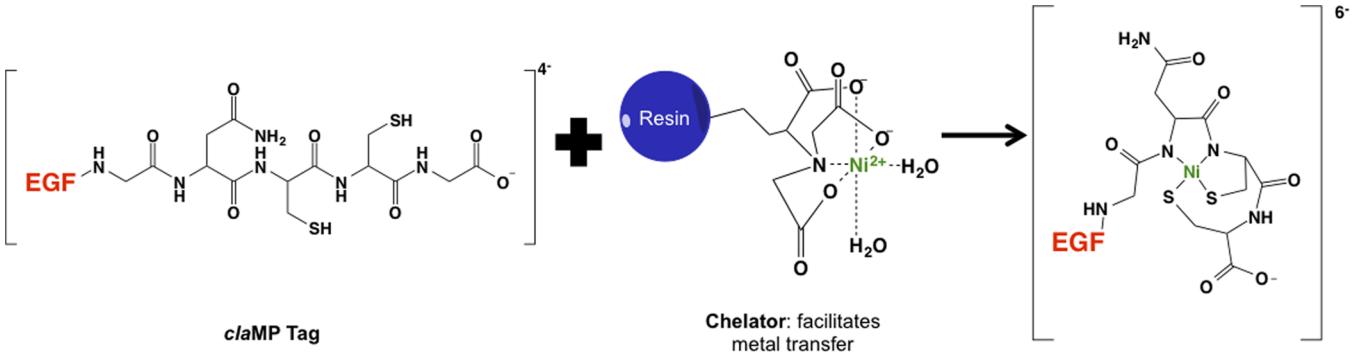


**Figure 1.** Schematic that illustrates the unique method by which metal is inserted into the *cla*MP Tag. The *cla*MP Tag is reacted with a chelated metal ion (i.e., Ni-NTA), which leads to metal insertion into the tag. A metal ion with a $2^+$ charge, such as Ni(II), reacted with the net neutral *cla*MP Tag sequence generates a single product with a charge of $2^-$. EGF has a $4^-$ charge, resulting in a net charge of $6^-$ for the inline *cla*MP Tag conjugate.

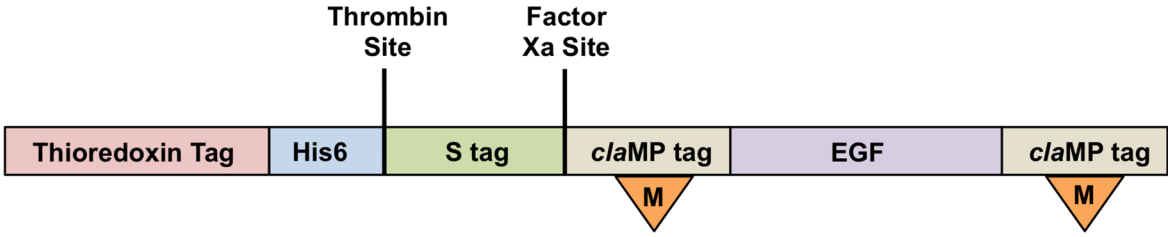


**Figure 2.** Cartoon of pET-32 expression construct of recombinant *cla*MP-Tagged EGF.

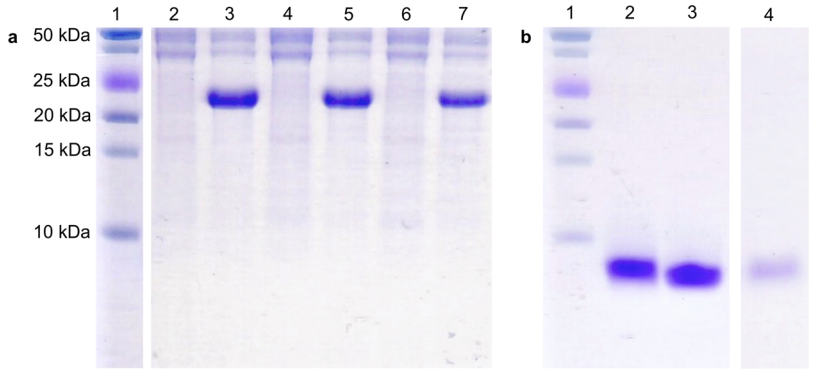


**Figure 3.** Addition of *cla*MP Tag to EGF did not significantly hinder expression or purification of desired product. Coomassie stained 18% tris-tricine gels illustrating the expression of pET-32-EGF, pET-32-*cla*MP-EGF, and pET-32-EGF-*cla*MP and final purified EGF products. (a) (Lane 1) molecular weight standard, (lanes 2, 4, 6) *E. coli* lysate of pET-32-EGF, pET-32-*cla*MP-EGF, and pET-32-EGF-*cla*MP before IPTG induction, (lanes 3, 5, 7) *E. coli* lysate of pET-32-EGF, pET-32-*cla*MP-EGF, and pET-32-EGF-*cla*MP 16 h after IPTG induction. (b) (Lane 1) molecular weight standard, (lane 2) purified EGF-Ni-*cla*MP, (lane 3) purified EGF, and (lane 4) purified Ni-*cla*MP-EGF.

composed of a three amino acid sequence (Asn-Cys-Cys; NCC), and when positioned inline, the metal is coordinated in a square planar organization by two thiolate ligands and two deprotonated amide nitrogens from the peptide backbone.[19] Because the sequence is composed of natural amino acids, it can be engineered as a tag into a genetic construct. The desired protein product encodes the inline metal carrier, which we refer to as the *cla*MP Tag. In order to generate the specific metal-bound peptide structure having these unique properties, the *cla*MP Tag must be reacted with a metal ion that is partially coordinated by a chelator (Figure 1), such as those used in immobilized metal affinity chromatography (IMAC), e.g., nitrilotriacetic acid (NTA). The peptide abstracts the metal ion from the high-affinity chelator; this reaction is extremely efficient and yields a highly stable, single product.[19−21]

Here, epidermal growth factor (EGF) was used as a model system to demonstrate that the *cla*MP sequence can be used effectively as a tag. EGF contains six cysteine residues, which comprise three disulfide bonds, and its expression is known to require the assistance of disulfide modulating enzymes to fold correctly.[22−25] Because the *cla*MP Tag itself contains two cysteine residues, these additional thiols could complicate the folding process by increasing the number of possible folded states. EGF was chosen because it exemplifies the extremes of protein systems to which the *cla*MP Tag may be applied. Production of EGF as a thioredoxin-fusion protein was performed to assess the ability to include the *cla*MP Tag in a thiol- and disulfide-containing fusion protein. Because the Ni-MAP complex has catalytic superoxide dismutase activity,[19] SOD activity of Ni-*cla*MP EGF can be used to cross-validate formation of the desired product. Here, the effects of the tag and its placement within EGF on expression, structure, and native function of EGF are presented to demonstrate the


dx.doi.org/10.1021/bc500115h | *Bioconjugate Chem.* 2014, 25, 1103−1111

compatibility and versatility of the *cla*MP Tag for use as an inline metal carrier.

## RESULTS

***cla*MP Tag Addition Does Not Impair EGF Expression.** Because native EGF contains three disulfide bonds, it was important to determine the extent to which addition of the two cysteine residues in the *cla*MP Tag might affect protein expression or lead to non-native disulfide bond formation and misfolding in an *E. coli* system. Native EGF, like many disulfide-containing proteins, accumulates in inclusion bodies when expressed into the reducing cytosolic environment of *E. coli*,[24,26] and addition of the *cla*MP Tag did not affect this outcome (unpublished data). By expressing EGF in an engineered strain that contains a more oxidizing cytoplasmic environment, proper folding is achieved (Figure 2).[27,28] Using this approach, EGF and *cla*MP-Tagged EGF variants were produced in the soluble fraction of the cell lysate.

SDS-PAGE was used to verify the *cla*MP Tag did not adversely affect expression of *cla*MP-Tagged EGF; all EGF variants showed excellent expression and reasonably similar expression levels (Figure 3a). The molecular weight of each fusion protein was expected to be approximately 24 kDa. As shown in Figure 3a, no band is present at this size in the preinduction samples (lanes 2, 4, and 6), but a band appears in the postinduction sample for each of the various constructs (lanes 3, 5, and 7), confirming successful expression. Native EGF was used as a standard to establish relative expression of the *cla*MP-Tagged forms. N-terminal and C-terminal placement led to a 14% and 29% decrease in EGF expression yield, respectively. Differences in expression among the variants were on the same order as batch-to-batch variation among replicates of the same protein. Therefore, insertion of the *cla*MP Tag into the protein sequence has a negligible effect on protein expression, as determined by densitometric analysis of whole cell lysates.

***cla*MP-Tagged EGF Is Soluble.** The EGF variants accumulated in the soluble fraction of the cell lysate, as determined by SDS-PAGE analysis of the supernatant and pellet from each sample following centrifugation of the lysate (data not shown). Following individual processing and purification steps, the yield of each protein variant was determined (Table 1). SDS-PAGE was performed to examine the purity and amount of protein present at each step, and the pure final product is shown in Figure 3b. Cleavage of the fusion tags from EGF-*cla*MP worked as expected, completely cleaving the fusion protein and yielding the expected amount of each product. During Factor Xa cleavage, a 30% lower yield was observed with the N-terminally tagged construct in comparison to EGF-Ni-*cla*MP (Table 1). The *cla*MP Tag abuts the Factor Xa recognition sequence, and therefore, it is hypothesized that cleavage efficiency is reduced because the Ni-*cla*MP complex kinks the protein conformation near the site, limiting access by the protease to the cleavage site. Sample purity of the final EGF proteins also was assessed using size exclusion chromatography (Figure 4). As a control, native EGF was examined, and it elutes at 12 min. EGF-Ni-*cla*MP elutes earlier than EGF at 10 min, which is expected because it is slightly larger than EGF.

***cla*MP-Tagged EGF Is Correctly Folded.** The three disulfide bonds present in EGF are the primary contributing factors to the protein structure. As such, conservation of the native disulfide bonds is essential to preserve protein structure and maintain biological function. Formation of the native

**Table 1. Relative Yields of EGF Constructs**

| conjugate | Trx-EGF (mg) | EGF mass equivalents (mg)[a] | EGF mass before final cleavage (mg)[b] | final product (mg) | % yield[c] | average percent yield |
|---|---|---|---|---|---|---|
| **EGF** | 11.8 | 3.1 | 2.6 | 1.2 | 46% | 53 ± 7% |
| | 7.6 | 2.0 | 1.3 | 0.7 | 60% | |
| **EGF-Ni-*cla*MP** | 6.9 | 1.9 | 2.3 | 1.1 | 45% | |
| | 15.1 | 4.2 | 4.8 | 1.6 | 34% | 43 ± 7% |
| | 12 | 3.3 | 3.0 | 1.5 | 50% | |
| **Ni-*cla*MP-EGF** | 8.2 | 2.3 | 3.2 | 0.5 | 14% | 12 ± 3% |
| | 7.2 | 2.0 | 1.7 | 0.1 | 9% | |

[a]The mass of EGF within the fusion protein was determined by taking into account the molecular weight of the fusion protein and EGF in the construct. [b]The mass of EGF within the fusion protein was determined by taking into account the molecular weight of the remaining portion of the fusion tags and EGF in the construct. [c]Percent yield was determined by comparing the final yield to the theoretical amount of EGF before the final cleavage step. The second cleavage step was used to determine the percent yield.

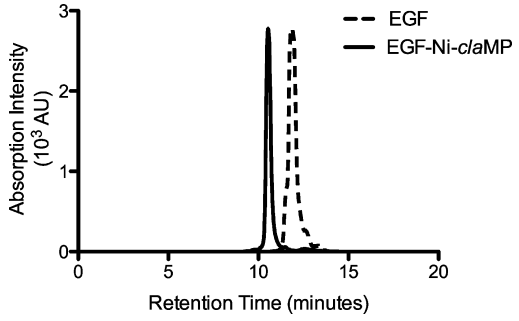


**Figure 4.** Size-exclusion chromatography verifies that one main species is present in the sample. EGF-Ni-*cla*MP elutes slightly earlier than EGF.

disulfide bonds in EGF occurs through multiple iterations of incorrect cysteine pairs until the correct disulfide network is achieved,[29] and addition of the *cla*MP Tag introduces two additional non-native cysteine residues into EGF, which could interfere with the native disulfide network. To validate that addition of the *cla*MP Tag to EGF did not affect protein structure, two-dimensional heteronuclear NMR was used to compare the variants to native EGF (Figure 5).[27] A $^{1}H-^{15}N$ HSQC spectrum provides a fingerprint of the protein; each amide from the backbone generates one peak, which reflects the unique conformation of the corresponding residue within the structured protein. $^{1}H-^{15}N$ HSQC spectra obtained for EGF and EGF-Ni-*cla*MP are highly similar and have specific, localized differences. The spectra show that the native fold of the protein is maintained in the presence of the *cla*MP Tag, as the majority of the residues in both spectra overlay. The disulfide network is also maintained; the chemical shift positions of the five assigned cysteine residues remain unperturbed. The data show that the tertiary structure is not altered by the addition of the *cla*MP Tag. In the EGF-Ni-*cla*MP spectrum, a few notable differences from native EGF are observed; residues near the C-terminus of the protein (K48, W49/50, L52, and R53) are shifted. There also are differences in peak intensity observed between the variants for M21, G36,


dx.doi.org/10.1021/bc500115h | *Bioconjugate Chem.* 2014, 25, 1103−1111

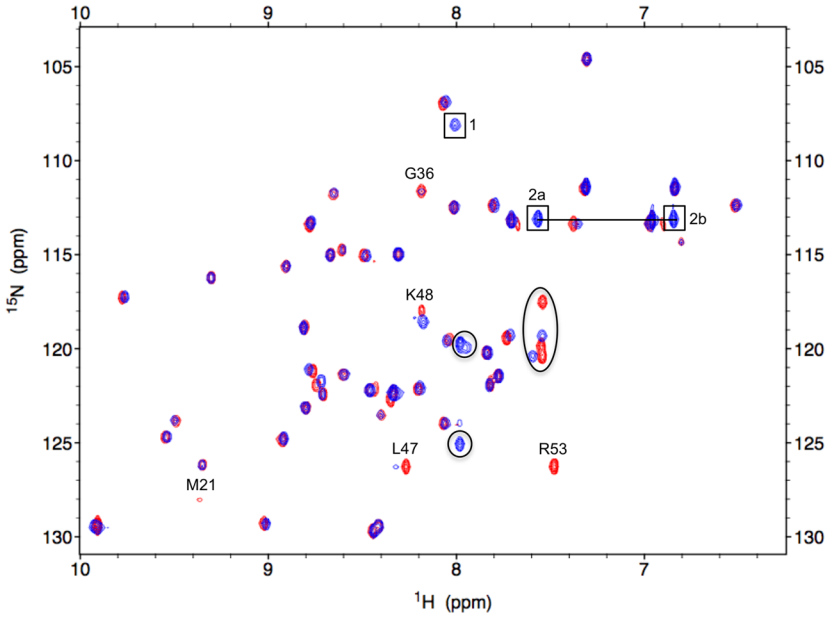


**Figure 5.** Higher order protein structure is maintained in the presence of *cla*MP Tag. $^{1}$H−$^{15}$N HSQC spectra of EGF (red) and EGF-Ni-*cla*MP (blue) at 0.1 mM and 0.08 mM, respectively. Peaks from native EGF that decrease in intensity when the tag is present are labeled with their corresponding residues. Shifted peaks corresponding to C-terminal residues are circled. New peaks 1, 2a, and 2b appear due to the addition of the *cla*MP Tag. Peak 1 corresponds to a glycine residue and Peaks 2a and 2b correspond to the asparagine side chain amide.

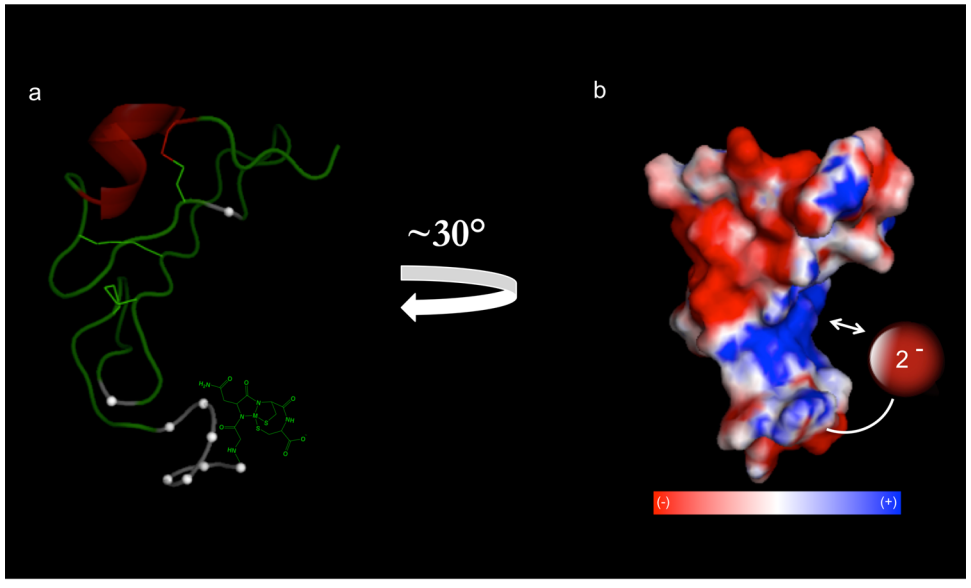


**Figure 6.** Illustration of the potential location of Ni-*cla*MP within the EGF molecule. (a) Schematic of EGF molecule; residues affected by addition of the *cla*MP Tag on the C-terminus are shown in gray. (b) Electrostatic surface map of EGF with the Ni-*cla*MP Tag added onto the C-terminus. The negatively charged Ni-*cla*MP complex is hypothesized to associate with the positively charged pocket shown in blue.

and L47. Because NMR is exquisitely sensitive to small changes in local environment, the presence of the metal-bound *cla*MP Tag would be expected to influence the chemical shift of neighboring residues. The chemical shift positions of EGF with and without the tag were compared and the differences mapped onto the structure of EGF to show the residues affected by the tag. The structure reveals that the negatively charged Ni-*cla*MP module likely associates with a neighboring patch of positive charge (Figure 6).

In addition, three peaks emerge in the EGF-Ni-*cla*MP spectrum, which may be due to the addition of residues composing the tag. We expect Peak 1 to correspond to the amide backbone of one of the glycine residues because it appears in the glycine region.[30] The backbone of the asparagine and first cysteine residues do not generate peaks because the *cla*MP Tag binds to the metal via these nitrogens, deprotonating them. The other two residues do not generate observable peaks in the HSQC. The asparagine side chain from the tag is visible in the spectrum, and it appears as a new pair of peaks with unique $^{1}$H values and the same $^{15}$N chemical shift (Peaks 2a, 2b).

**Ni(II) Is Selectively Inserted into *cla*MP Tag in the Presence of EGF.** For the initial analytical development, Ni(II) was used to occupy the *cla*MP Tag because this is a well


dx.doi.org/10.1021/bc500115h | *Bioconjugate Chem.* 2014, 25, 1103−1111

understood system in our lab.[19−21] Insertion of Ni(II) into the *cla*MP Tag can be accomplished using Ni(II)-charged IMAC resin or via solution transfer using aqueous Ni-NTA,[19−21] both resulting in formation of the desired Ni-*cla*MP complex. The *cla*MP-Tagged EGF was produced as a His-tagged fusion protein, which accomplished affinity purification and facilitated complete Ni(II) transfer into the *cla*MP Tag during the purification process. Use of IMAC resin for transfer very efficiently limits nonspecific binding of Ni(II) to proteins. EGF has previously been purified using Ni(II)-based affinity chromatography, and Ni(II) was not reported to nonspecifically bind to EGF.[27] Control reactions performed with native protein in this study confirm this result.

The Ni-*cla*MP complex of the correct structure has a rusty orange color, allowing incorporation in the context of the protein to be confirmed with absorption spectroscopy, as established with the peptide system.[21] In the EGF-Ni-*cla*MP spectrum, there are broad features present in the visible region that reflect the structure of the unique metal complex, as seen in Figure 7a. These features are absent from the control spectrum of native EGF, which confirms they are due to correct Ni-*cla*MP formation and not nonspecific binding of Ni(II) to EGF.

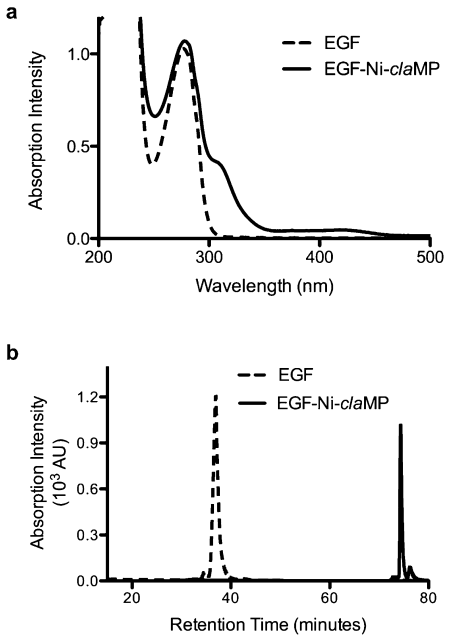


**Figure 7.** Ni(II) is successfully incorporated into the *cla*MP Tag in the presence of EGF. (a) Absorption spectroscopy validates Ni(II) incorporation into the *cla*MP Tag. In comparison to EGF, EGF-Ni-*cla*MP contains distinct features in the visible region, which confirm Ni(II) incorporation. (b) Anion exchange chromatography demonstrates the difference in net charge between EGF and EGF-Ni-*cla*MP due to the addition of Ni-*cla*MP.

AEC also was used to verify that proper formation of the Ni-*cla*MP complex was achieved. Correct incorporation of Ni(II) into the *cla*MP Tag creates a net charge of $2^-$. Native and metal-free *cla*MP-Tagged EGF each have an overall charge of $4^-$, but proper nickel insertion into *cla*MP-Tagged EGF develops an overall charge of $6^-$. This difference in charge results in unique AEC elution profiles for the two species. As shown in Figure 7b, EGF elutes at 35 min, whereas EGF-Ni-*cla*MP elutes at 75 min. The greater negative charge of EGF-Ni-*cla*MP causes it to bind more strongly to the cationic resin allowing AEC to be utilized to confirm metal binding and to separate the two distinct charge species.

As it has been shown that the Ni-*cla*MP complex acts as a superoxide mimic,[19] verification of complex formation in the presence of EGF can be confirmed using a standard SOD activity assay. The $IC_{50}$ values for the Ni-MAP module and EGF-Ni-*cla*MP are 35 ± 8 $\mu$M and 44 ± 4 $\mu$M, respectively, which are comparable within experimental error for the xanthine/xanthine oxidase assay. This confirms that the Ni-*cla*MP Tag specifically and efficiently forms the unique structure determined for the original Ni-MAP module and this module maintains comparable SOD-like activity in the context of the protein.

**EGF Remains Functional with Addition of *cla*MP Tag.** In order to be used successfully as an inline metal carrier, the *cla*MP Tag cannot be deleterious to the function of the protein. A standard cell viability assay using the A431 cell strain was completed to assess the impact of the *cla*MP Tag on EGF function. This strain is known for its overexpression of the epidermal growth factor receptor (EGFR) on the cell surface.[31] Overexpression of EGFR leads to the unexpected outcome of growth inhibition upon stimulation with EGF.[31] The N- and C-termini of EGF are not responsible for high-affinity binding to the receptor,[32] so placement of the *cla*MP Tag on either terminus would not be expected to diminish EGF activity, and indeed it does not. EGF or either *cla*MP-Tagged variant of EGF elicits a similar cytostatic response (Figure 8). At nanomolar

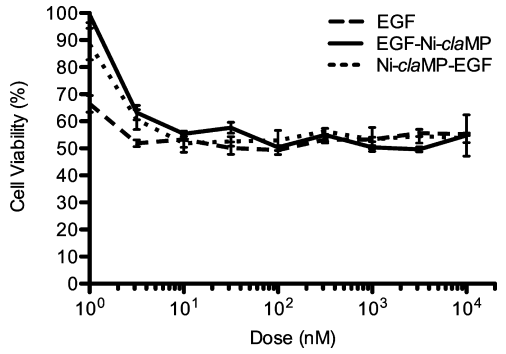


**Figure 8.** Addition of the *cla*MP Tag to either the N- or C-terminus of EGF has little to no effect on the function of the protein. The decrease in cell viability of A431 cells caused by addition of EGF is comparable to that of both Ni-*cla*MP-EGF and EGF-Ni-*cla*MP.

concentrations, addition of EGF or either Ni-*cla*MP-EGF protein results in a 50% loss in cell viability in the A431 cell line, confirming EGF remains active in the presence of the tag at either position.

## DISCUSSION

Metal-binding agents enable a wide range of biotechnology, healthcare, and research applications. Peptide tags and organic molecules capable of binding metal ions can be combined with the appropriate protein to allow for targeted delivery of metal ions for imaging and therapeutic applications and for use as analytical research tools.[3,8,10,33−35] Incorporation of a metal-binding tag into a protein can be accomplished using either chemical conjugation or inline addition. Conjugation is typically performed using chemical means, primarily conjugation to lysine or cysteine residues using moiety specific chemis-


dx.doi.org/10.1021/bc500115h | *Bioconjugate Chem.* 2014, 25, 1103−1111

try,[3−5,36,37] which can have adverse effects on protein structure due to the heterogeneity associated with this type of conjugation.[38−40] With chemical conjugation, protein function may also be altered because the exact attachment site cannot be controlled,[41] and lysine residues are often present in receptor recognition sites of many proteins, including antibodies.[42,43] In addition, in vivo PK may be affected.[44] For example, modification of the Fc region can alter binding to FcRn, resulting in changes in biodistribution, endosomal recycling, and PK.[45] The *cla*MP Tag is similar in size to small chelating agents, but it bears the added advantage that it can be inserted inline with the protein sequence using standard cloning methodologies, allowing precise control of its placement. Site-specific placement of the *cla*MP Tag within EGF allows for correct folding and disulfide-bond formation, confirming that precise placement of the *cla*MP Tag can be used to generate a bioconjugate that retains native structural elements and, importantly, its functionality. The *cla*MP Tag is advantageous in that its location can be specifically modulated, allowing for the generation of an inline metal carrier that can be precisely positioned to avoid disrupting protein properties.

While chelators have been developed that bind transition metals, their properties are often incompatible with clinical use. Tight binding chelators to copper have been developed, but those with sufficiently slow off rates for in vivo use require very high temperature and long incubation times to accomplish binding. SarAr technology is an exception, which achieves tight binding under reasonable conditions for use with proteins,[46] but this chelator is selective for and only used with copper.[47] The *cla*MP Tag is capable of binding a wide range of transition metals, including many species that are used to enable imaging and therapeutic applications, under conditions amenable to retention of higher-order protein structure. Cytotoxic metal ions, such as Pt or Pd, can be loaded into the *cla*MP Tag and have the potential to be used in targeted oncology applications (manuscripts in preparation). Radioactive tracer metals, such as $^{99m}$Tc, $^{55}$Co, $^{64/67}$Cu, or $^{212}$Pb, also can be incorporated into the tag (manuscripts in preparation), and these isotopes have proven utility in diagnostic imaging.[48−54] As shown here, Ni(II) can be selectively inserted into the tag even when placed in a protein sequence, and though not currently in wide usage, $^{57}$Ni could be substituted and monitored based on its positron or X-ray emission.[55,56] Ni-*cla*MP has been shown to act as catalytic antioxidant,[19−21] and the Ni-*cla*MP complex retains that activity in the context of a protein system. This catalytic activity of a Ni(II)-*cla*MP Tag conjugate may be useful in the generation of a targeted anti-inflammatory agent or as a biotechnology reagent for selective detection of tagged proteins.

## CONCLUSION

In order to investigate the potential of using the *cla*MP Tag as an inline metal carrier, its effects on the expression, structure, and function of a thiol- and disulfide-containing protein and metal insertion into the tag were analyzed. The spectroscopic and chromatographic data verify that incorporation of Ni(II) into the *cla*MP Tag is not affected when the tag is placed inline with a protein sequence. The overall structure of *cla*MP-Tagged EGF is also maintained, as the chemical shift positions of the native cysteine residues remain unaltered. In addition, native function is maintained with *cla*MP Tag inclusion at either terminus. The study described here demonstrates successful inline incorporation of the *cla*MP Tag into a protein, illustrating that this tag provides opportunity to expand the range of applications in which metals may be used in biotechnology and healthcare.

## MATERIALS AND METHODS

**Cloning and Construction of the Expression Plasmid.** Three DNA sequences were prepared to generate EGF variants: control EGF and two individually tagged variants containing the *cla*MP Tag at either the N-terminus (GNCCG-EGF) or C-terminus (EGF-GNCCG) of the native sequence. A plasmid containing human EGF was obtained (Origene, #RC210817), and the EGF sequence was amplified using PCR and subcloned into the pET-32Xa/LIC vector. GNCCG was added to either the N-terminus or C-terminus of EGF and amplified using PCR for insertion into a LIC plasmid using the primers below (IDT). In each primer, the LIC sequence is underlined and the portion corresponding to EGF and the *cla*MP Tag are not. 5′-GGTATTGAGGGTCGCGGAAA-CTGCTGCGGCAATAGTGACTCTGAATGTCCC-3′ (forward primer with tag on the N-terminus), 5′-AGAGGAG-AGTTAGAGCCGTCAGCGCAGTTCCCACCACTTCAG-3′ (reverse primer for N-terminally tagged construct), 5′-GGT-ATTGAGGGTCGCAATAGTGACTCTGAATGTCCC-CTGTCCCACGATGGG (forward primer for C-terminal tagged construct), and 5′-AGAGGAGAGTTAGAGCCG-TCAGCCGCAGCAGTTTCCGCGCAGTTCCCACCACTT-CAGGTC-3′ (reverse primer with tag on the C-terminus). The amplification reactions were purified using the QIAquick PCR Purification Kit (Qiagen). The fragments were inserted into the vector using the manufacturer's protocol from the Xa/LIC cloning kit (Novagen). These plasmids contain a Thioredoxin tag, a His6 tag, thrombin cleavage site, S-tag, and Factor Xa site, which are all positioned on the N-terminal side of each EGF variant (Figure 2). The ligation product was transformed into the DH5$\alpha$ *Escherichia coli* cell strain using the standard heat shock method, and the DNA was harvested after selection and growth on LB containing 100 $\mu$g/mL ampicillin. Plasmid DNA was purified using a miniprep kit (Qiagen), and the intended product was verified by DNA sequencing (UC Berkeley DNA Sequencing Facility).

**Protein Expression.** Expression and purification of the protein from these plasmids was completed in a similar manner to that previously reported for EGF.[27] Each plasmid was transformed into the Origami B (DE3) *E. coli* strain (Novagen) using the standard heat shock protocol. Colonies were grown for ~24 h at 37 °C on LB agar plates with 100 $\mu$g/mL ampicillin, 30 $\mu$g/mL kanamycin, and 12.5 $\mu$g/mL tetracycline. To prepare $^{15}$N-labeled cultures, individual colonies were selected to inoculate 175 mL M9ZB media supplemented with 0.4% glucose, 1 mM $MgSO_4$, and 100 $\mu$g/mL ampicillin. These starter cultures were grown for 16 h at 37 °C, 250 rpm. Fifty milliliters of starter culture was used to inoculate 1 L minimal media containing minimal salts and trace minerals.[57] To prepare nonlabeled cultures, individual colonies were selected to inoculate 50 mL LB media containing 100 $\mu$g/mL ampicillin. Again, starter cultures were grown for 16 h at 37 °C, 250 rpm. Twenty milliliter starter culture was used to inoculate 1 L LB supplemented with 100 $\mu$g/mL ampicillin. Cultures of $^{15}$N-labeled media and nonlabeled media were allowed to incubate at 200 rpm and 37 °C until an $OD_{600}$ of 0.7 was met. At this point, protein expression was induced through the addition of 1 mM isopropyl $\beta$-D-1-thiogalactopyranoside (IPTG). The cultures were allowed to incubate for an additional 16 h at

25 °C, 200 rpm, and then they were harvested by ultracentrifugation. Cell pellets were stored at −80 °C until use.

**Protein Purification.** Each pellet (1 L of culture) was resuspended in 25 mL 50 mM Tris-Cl, 20 mM imidazole, pH 7.9, and lysed using a French Press at 21 000 psi. The cellular debris was removed by centrifugation at 21 000*g* for 1 h at 4 °C. The supernatant, which contained the protein, was filtered through a 0.45 μm filter and applied to a 5 mL Hi-Trap Chelating HP column charged with nickel (GE Lifesciences). EGF constructs containing the *cla*MP Tag were allowed to incubate on the column for 1 h to facilitate metal transfer to the tag. Cellular proteins were removed by washing the column with six column volumes (CV) of 50 mM Tris-Cl, 40 mM imidazole, 500 mM NaCl, pH 7.9. The protein was eluted from the column using a linear gradient from 0% to 100% 20 mM sodium phosphate (NaPi), 500 mM NaCl, 500 mM imidazole, pH 9.5 over 12 CV. The thioredoxin tag was cleaved using 10 units thrombin (FisherScientific) per mg of protein at 16 °C for 9.5 h, and the two cleavage fragments were separated on a Superdex75 column (GE Lifesciences). The remaining tags were cleaved using 9 units Factor Xa (Novagen) per mg of protein at 25 °C for 16 h, and the two cleavage fragments were separated on a Superdex75 column. Samples were concentrated using an Amicon Ultra 3 kDa MWCO concentrator (Millipore) to a final concentration of approximately 0.15 mM. The purity of the protein was confirmed with SDS-PAGE and size exclusion chromatography (TSKgel G3000SW, 7.8 mm × 30 cm, 5 μm particle size, Fisher Scientific) and the molecular weight was validated with ESI-MS. Samples were quantified using a Bradford assay.

**SDS-PAGE Analysis.** Tris-tricine gels were prepared as reported.[58] EGF constructs were separated using a discontinuous system consisting of a 4% (v/v) stacking gel and a 18% (v/v) resolving gel. The samples were prepared in nonreducing Laemmli buffer and heated for 10 min at 90 °C before being loaded onto the gel. A prestained, dual-color molecular weight marker was used for reference (BioRad, #161−0374). Gels were stained using Coomassie (R-250).

Densitometry analysis was performed on Coomassie-stained tris-tricine gels using the Typhoon TRIO Variable Mode Imager (Amersham Biosciences). Relative quantitation was performed using the ImageQuantTL software (Amersham Biosciences). The amount of *cla*MP-Tagged EGF was determined based upon the intensity observed for native EGF.

**Absorption Analysis.** After purification, samples were diluted and analyzed using absorption spectroscopy to confirm Ni(II) incorporation. Samples were placed in a cuvette with a 1 cm path length and spectra were acquired from 200 to 800 nm using a Carey 100 Bio UV−visible spectrophotometer (Varian).

**HPLC Analysis.** Anion exchange chromatography (AEC) was performed on a 4 × 250 mm BioLC ProPac Wax10 column (Dionex). The column was equilibrated with 20 mM Tris-Cl, 10 mM KCl, pH 7.5 before injection of the sample. A linear gradient from 0% to 100% 20 mM Tris-Cl, 500 mM KCl, pH 7.5 over 70 mL with a constant flow rate of 1 mL/min was used to elute the protein from the column and detected by absorbance at 220 nm. The sample volume used for all injections was 20 μL, and each sample was run in duplicate.

**$^{1}$H−$^{15}$N HSQC Analysis.** Two-dimensional $^{1}$H−$^{15}$N heteronuclear single quantum coherence (HSQC) spectra were obtained at 25 °C using a 600 MHz Bruker Avance NMR spectrometer with a cryogenic, triple resonance probe. $^{15}$N-labeled protein was prepared in 50 mM KPi, 10 mM NaCl, pH 7.3, with 6% $D_2O$. A Bradford assay was used to determine the concentration of the samples. Data were obtained with 177 and 217 scans for EGF and EGF-Ni-*cla*MP, respectively. A different number of scans were used to account for variations in sample concentrations and achieve a similar signal-to-noise ratio for each 2D spectrum. Analysis of the data was performed using NMRPipe[59] and the NMR assignment program Sparky.[60]

**Xanthine/Xanthine Oxidase SOD Activity Assay.** This assay was performed as previously described.[19,61,62] Briefly, 600 μM cytochrome c from bovine heart and 300 μM xanthine were added to 50 mM potassium phosphate with 100 μM EDTA, pH 7.8 to yield final concentrations of 10 μM cytochrome c and 50 μM xanthine. Enough xanthine oxidase was added to cause a change in absorbance at 550 nm of 0.02 to 0.04 AU/min. Several concentrations were analyzed to develop an $IC_{50}$ curve.

**Cell Culture.** Human epidermoid carcinoma cells (A431, ATCC CRL-1555) were purchased from American Type Culture Collection (ATCC) and grown in Dulbecco's Modified Eagle's Medium (DMEM) supplemented with 10% fetal bovine serum and 1% penicillin and streptomycin. Cells were cultured in an incubator at a constant temperature of 37 °C and 5% $CO_2$.

**EGF Cell Viability Assay.** A431 cells were seeded in a 96-well clear bottom black plate at a density of 10 000 cells per well and incubated overnight in the growth conditions described above. The following day, the media was replaced with media containing the test samples and controls. Test samples were diluted into media at the appropriate concentrations and then transferred onto the cells. Nine different concentrations were used, and each sample was run in triplicate. The cells were incubated with EGF variants for 72 h, when the control cells reached confluency. Cell viability was measured using the CellTiter-Blue assay (Promega) following manufacturer's protocol. Briefly, the media was replaced with cell culture medium containing reagent and allowed to incubate for 30 min. Following this incubation period, a microplate reader (SpectraMax GeminiXS) was used to determine the fluorescence intensity of the dye ($560_{ex}/590_{em}$). The fluorescence intensity was compared to control wells to determine percent viability.

## AUTHOR INFORMATION

### Corresponding Author

*Tel.: 785-864-3405, Fax: 785-864-5736, E-mail: laurencj@ku.edu.

### Notes

The authors declare the following competing financial interest(s): J.S.L. is co-owner of Echogen Inc., which has licensed the patent-protected MAP Tag technology from the University of Kansas.

## ACKNOWLEDGMENTS

Funding was provided by Wallace H. Coulter Foundation (CTRA) and KU Cancer Center Pilot Award. NIGMS Biotechnology Predoctoral Training Grant (T32 GM-08359) provided support for B.J.M. M.E.K. was supported by a PhRMA Foundation Postdoctoral Fellowship. The authors thank Heather Shinogle at KU Microscopy and Imaging Laboratory for use of equipment and assistance with densitometry analysis and the KU Mass Spectrometry lab for running the mass spectrometry samples and assistance with data analysis.

## ■ ABBREVIATIONS

MAP, metal abstraction peptide; EGF, epidermal growth factor; LBTs, lanthanide-binding tags; EDTA, ethylenediaminetetraacetic acid; IMAC, immobilized metal affinity chromatography; NTA, nitrilotriacetic acid; SOD, superoxide dismutase; *E. coli*, *Escherichia coli*; HSQC, heteronuclear single quantum correlation; AEC, anion exchange chromatography; NaPi, sodium phosphate; SEC, size exclusion chromatography; EGFR, epidermal growth factor receptor; PK, pharmacokinetics; NMR, nuclear magnetic resonance; LIC, ligation independent cloning; IPTG, Isopropyl $\beta$-D-1-thiogalactopyranoside; CV, column volumes; SDS-PAGE, sodium dodecyl sulfate polyacrylamide gel electrophoresis; KPi, potassium phosphate

## ■ REFERENCES


(1) Aoki, I., Takahashi, Y., Chuang, K.-H., Silva, A. C., Igarashi, T., Tanaka, C., Childs, R. W., and Koretsky, A. P. (2006) Cell labeling for magnetic resonance imaging with the T1 agent manganese chloride. *NMR Biomed. 19*, 50−59.

(2) Zheng, Q., Dai, H., Merritt, M. E., Malloy, C., Pan, C. Y., and Li, W.-H. (2005) A new class of macrocyclic lanthanide complexes for cell labeling and magnetic resonance imaging applications. *J. Am. Chem. Soc. 127*, 16178−16188.

(3) De León-Rodríguez, L. M., and Kovacs, Z. (2008) The synthesis and chelation chemistry of DOTA-peptide conjugates. *Bioconjugate Chem. 19*, 391−402.

(4) Lewis, M. R., Kao, J. Y., Anderson, A.-L. J., Shively, J. E., and Raubitschek, A. (2001) An improved method for conjugating monoclonal antibodies with N-Hydroxysulfosuccinimidyl DOTA. *Bioconjugate Chem. 12*, 320−324.

(5) Lewis, M. R., Raubitschek, A., and Shively, J. E. (1994) A facile, water-soluble method for modification of proteins with DOTA. Use of elevated temperature and optimized pH to achieve high specific activity and high chelate stability in radiolabeled immunoconjugates. *Bioconjugate Chem. 5*, 565−576.

(6) Knör, S., Modlinger, A., Poethko, T., Schottelius, M., Wester, H.-J., and Kessler, H. (2007) Synthesis of novel 1,4,7,10-tetraazacyclodecane-1,4,7,10-tetraacetic acid (DOTA) derivatives for chemoselective attachment to unprotected polyfunctionalized compounds. *Chem.—Eur. J. 13*, 6082−6090.

(7) Franz, K. J., Nitz, M., and Imperiali, B. (2003) Lanthanide-binding tags as versatile protein coexpression probes. *ChemBioChem 4*, 265−271.

(8) Martin, L. J., Hähnke, M. J., Nitz, M., Wöhnert, J., Silvaggi, N. R., Allen, K. N., Schwalbe, H., and Imperiali, B. (2007) Double-lanthanide-binding tags: design, photophysical properties, and NMR applications. *J. Am. Chem. Soc. 129*, 7106−7113.

(9) Nitz, M., Sherawat, M., Franz, K. J., Peisach, E., Allen, K. N., and Imperiali, B. (2004) Structural origin of the high affinity of a chemically evolved lanthanide-binding peptide. *Angew. Chem., Int. Ed. 43*, 3682−3685.

(10) Sculimbrene, B. R., and Imperiali, B. (2006) Lanthanide-binding tags as luminescent probes for studying protein interactions. *J. Am. Chem. Soc. 128*, 7346−7352.

(11) Wöhnert, J., Franz, K. J., Nitz, M., Imperiali, B., and Schwalbe, H. (2003) Protein alignment by a coexpressed lanthanide-binding tag for the measurement of residual dipolar couplings. *J. Am. Chem. Soc. 125*, 13338−13339.

(12) Yang, J. J., Yang, J., Wei, L., Zurkiya, O., Yang, W., Li, S., Zou, J., Zhou, Y., Wilkins Maniccia, A. L., Mao, H., Zhao, F., Malchow, R., Zhao, S., Johnson, J., Hu, X., Krogstad, E., and Liu, Z.-R. (2008) Rational design of protein-based MRI contrast agents. *J. Am. Chem. Soc. 130*, 9260−9267.

(13) Perazella, M. A. (2007) Nephrogenic systemic fibrosis, kidney disease, and gadolinium: is there a link? *Clin. J. Am. Soc. Nephrol. 2*, 200−202.

(14) Wadas, T. J., Wong, E. H., Weisman, G. R., and Anderson, C. J. (2010) Coordinating radiometals of copper, gallium, indium, yttrium, and zirconium for PET and SPECT imaging of disease. *Chem. Rev. (Washington, DC, U. S.) 110*, 2858−2902.

(15) McQuade, P., Miao, Y., Yoo, J., Quinn, T. P., Welch, M. J., and Lewis, J. S. (2005) Imaging of melanoma using 64Cu- and 86Y-DOTA-ReCCMSH(Arg11), a cyclized peptide analogue of $\alpha$-MSH. *J. Med. Chem. 48*, 2985−2992.

(16) Chen, X., Hou, Y., Tohme, M., Park, R., Khankaldyyan, V., Gonzales-Gomez, I., Bading, J. R., Laug, W. E., and Conti, P. S. (2004) Pegylated Arg-Gly-Asp peptide: 64Cu labeling and PET imaging of brain tumor $\alpha v\beta 3$-integrin expression. *J. Nucl. Med. 45*, 1776−1783.

(17) Ping, L. W., Lewis, J. S., Kim, J., Bugaj, J. E., Johnson, M. A., Erion, J. L., and Anderson, C. J. (2002) DOTA-D-Tyr1-octreotate: a somatostatin analogue for labeling with metal and halogen radionuclides for cancer imaging and therapy. *Bioconjugate Chem. 13*, 721−728.

(18) Laurence, J. A. S., Vartia, A. A., and Krause, M. E. Metal abstraction peptide (MAP) tag and associated methods. Singapore Patent 166345, June 29, 2012.

(19) Krause, M. E., Glass, A. M., Jackson, T. A., and Laurence, J. S. (2010) Novel tripeptide model of nickel superoxide dismutase. *Inorg. Chem. 49*, 362−364.

(20) Krause, M. E., Glass, A. M., Jackson, T. A., and Laurence, J. S. (2011) MAPping the chiral inversion and structural transformation of a metal-tripeptide complex having Ni-superoxide dismutase activity. *Inorg. Chem. 50*, 2479−2487.

(21) Krause, M. E., Glass, A. M., Jackson, T. A., and Laurence, J. S. (2013) Embedding the Ni-SOD mimetic Ni-NCC within a polypeptide sequence alters the specificity of the reaction pathway. *Inorg. Chem. 52*, 77−83.

(22) Chang, J.-Y., Schindler, P., Ramseier, U., and Lai, P.-H. (1995) The disulfide folding pathway of human epidermal growth factor. *J. Biol. Chem. 270*, 9207−9216.

(23) Lee, J. Y., Yoon, C. S., Chung, I. Y., Lee, Y. S., and Lee, E. K. (2000) Scale-up process for expression and renaturation of recombinant human epidermal growth factor from Escherichia coli inclusion bodies. *Biotechnol. Appl. Biochem. 31*, 245−248.

(24) Le, P. U., Lenferink, A. E. G., Pinard, M., Baardsnes, J., Massie, B., and O'Connor-McCourt, M. D. (2009) Escherichia coli expression and refolding of E/K-coil-tagged EGF generates fully bioactive EGF for diverse applications. *Protein Express. Purif. 64*, 108−117.

(25) Wu, J., Yang, Y., and Watson, J. T. (1998) Trapping of intermediates during the refolding of recombinant human epidermal growth factor (hEGF) by cyanylation, and subsequent structural elucidation by mass spectrometry. *Protein Sci. 7*, 1017−1028.

(26) Sharma, K., Cherish Babu, P. V., Sasidhar, P., Srinivas, V. K., Krishna Mohan, V., and Krishna, E. (2008) Recombinant human epidermal growth factor inclusion body solubilization and refolding at large scale using expanded-bed adsorption chromatography from Escherichia coli. *Protein Express. Purif. 60*, 7−14.

(27) Huang, H.-W., Mohan, S. K., and Yu, C. (2010) The NMR solution structure of human epidermal growth factor (hEGF) at physiological pH and its interactions with suramin. *Biochem. Biophys. Res. Commun. 402*, 705−710.

(28) Hammarström, M., Hellgren, N., Van Den Berg, S., Berglund, H., and Härd, T. (2002) Rapid screening for improved solubility of small human proteins produced as fusion proteins in Escherichia coli. *Protein Sci. 11*, 313−321.

(29) Chang, J.-Y., Li, L., and Lai, P.-H. (2001) A major kinetic trap for the oxidative folding of human epidermal growth factor. *J. Biol. Chem. 276*, 4845−4852.

(30) Jacobsen, N. E. (2007) *NMR Spectroscopy Explained: Simplified Theory, Applications and Examples for Organic Chemistry and Structural Biology*, Wiley, Hoboken, NJ.

(31) Gill, G. N., and Lazar, C. S. (1981) Increased phosphotyrosine content and inhibition of proliferation in EGF-treated A431 cells. *Nature (London) 293*, 305−307.

(32) Ogiso, H., Ishitani, R., Nureki, O., Fukai, S., Yamanaka, M., Kim, J.-H., Saito, K., Sakamoto, A., Inoue, M., Shirouzu, M., and Yokoyama, S. (2002) Crystal structure of the complex of human epidermal growth factor and receptor extracellular domains. *Cell (Cambridge, MA, U. S.) 110*, 775−787.
(33) Daughtry, K. D., Martin, L. J., Sarraju, A., Imperiali, B., and Allen, K. N. (2012) Tailoring encodable lanthanide-binding tags as MRI contrast agents. *ChemBioChem 13*, 2567−2574.
(34) Breeman, W. A. P., Kwekkeboom, D. J., de Blois, E., de Jong, M., Visser, T. J., and Krenning, E. P. (2007) Radiolabelled regulatory peptides for imaging and therapy. *Anti-Cancer Agents Med. Chem. 7*, 345−357.
(35) Wängler, C., Buchmann, I., Eisenhut, M., Haberkorn, U., and Mier, W. (2007) Radiolabeled peptides and proteins in cancer therapy. *Protein Pept. Lett. 14*, 273−279.
(36) Lewis, M. R., and Shively, J. E. (1998) Maleimidocysteineamido-DOTA derivatives: new reagents for radiometal chelate conjugation to antibody sulfhydryl groups undergo pH-dependent cleavage reactions. *Bioconjugate Chem. 9*, 72−86.
(37) Li, L., Tsai, S.-W., Anderson, A.-L., Keire, D. A., Raubitschek, A. A., and Shively, J. E. (2002) Vinyl sulfone bifunctional derivatives of DOTA allow sulfhydryl- or amino-directed coupling to antibodies. conjugates retain immunoreactivity and have similar biodistributions. *Bioconjugate Chem. 13*, 110−115.
(38) Adem, Y. T., Schwarz, K. A., Duenas, E., Patapoff, T. W., Galush, W. J., and Esue, O. (2014) Auristatin antibody drug conjugate physical instability and the role of drug payload. *Bioconjugate Chem. 25*, 656−664.
(39) Beckley, N. S., Lazzareschi, K. P., Chih, H.-W., Sharma, V. K., and Flores, H. L. (2013) Investigation into temperature-induced aggregation of an antibody drug conjugate. *Bioconjugate Chem. 24*, 1674−1683.
(40) Wakankar, A. A., Feeney, M. B., Rivera, J., Chen, Y., Kim, M., Sharma, V. K., and Wang, Y. J. (2010) Physicochemical stability of the antibody-drug conjugate Trastuzumab-DM1: changes due to modification and conjugation processes. *Bioconjugate Chem. 21*, 1588−1595.
(41) Shen, B.-Q., Xu, K., Liu, L., Raab, H., Bhakta, S., Kenrick, M., Parsons-Reponte, K. L., Tien, J., Yu, S.-F., Mai, E., Li, D., Tibbitts, J., Baudys, J., Saad, O. M., Scales, S. J., McDonald, P. J., Hass, P. E., Eigenbrot, C., Nguyen, T., Solis, W. A., Fuji, R. N., Flagella, K. M., Patel, D., Spencer, S. D., Khawli, L. A., Ebens, A., Wong, W. L., Vandlen, R., Kaur, S., Sliwkowski, M. X., Scheller, R. H., Polakis, P., and Junutula, J. R. (2012) Conjugation site modulates the in vivo stability and therapeutic activity of antibody-drug conjugates. *Nat. Biotechnol. 30*, 184−189.
(42) Bachran, C., Schneider, S., Riese, S. B., Bachran, D., Urban, R., Schellmann, N., Zahn, C., Sutherland, M., and Fuchs, H. (2011) A lysine-free mutant of epidermal growth factor as targeting moiety of a targeted toxin. *Life Sci. 88*, 226−232.
(43) Wang, Y.-J., Liu, Y.-D., Chen, J., Hao, S.-J., Hu, T., Ma, G.-H., and Su, Z.-G. (2010) Efficient preparation and PEGylation of recombinant human non-glycosylated erythropoietin expressed as inclusion body in E. coli. *Int. J. Pharm. 386*, 156−164.
(44) Boswell, C. A., Mundo, E. E., Zhang, C., Bumbaca, D., Valle, N. R., Kozak, K. R., Fourie, A., Chuh, J., Koppada, N., Saad, O., Gill, H., Shen, B.-Q., Rubinfeld, B., Tibbitts, J., Kaur, S., Theil, F.-P., Fielder, P. J., Khawli, L. A., and Lin, K. (2011) Impact of drug conjugation on pharmacokinetics and tissue distribution of anti-STEAP1 antibody-drug conjugates in rats. *Bioconjugate Chem. 22*, 1994−2004.
(45) Junutula, J. R., Raab, H., Clark, S., Bhakta, S., Leipold, D. D., Weir, S., Chen, Y., Simpson, M., Tsai, S. P., Dennis, M. S., Lu, Y., Meng, Y. G., Ng, C., Yang, J., Lee, C. C., Duenas, E., Gorrell, J., Katta, V., Kim, A., McDorman, K., Flagella, K., Venook, R., Ross, S., Spencer, S. D., Wong, W. L., Lowman, H. B., Vandlen, R., Sliwkowski, M. X., Scheller, R. H., Polakis, P., and Mallet, W. (2008) Site-specific conjugation of a cytotoxic drug to an antibody improves the therapeutic index. *Nat. Biotechnol. 26*, 925−932.
(46) Di Bartolo, N., Sargeson, A. M., and Smith, S. V. (2006) New 64Cu PET imaging agents for personalised medicine and drug development using the hexa-aza cage, SarAr. *Org. Biomol. Chem. 4*, 3350−3357.
(47) Voss, S. D., Smith, S. V., DiBartolo, N., McIntosh, L. J., Cyr, E. M., Bonab, A. A., Dearling, J. L. J., Carter, E. A., Fischman, A. J., Treves, S. T., Gillies, S. D., Sargeson, A. M., Huston, J. S., and Packard, A. B. (2007) Positron emission tomography (PET) imaging of neuroblastoma and melanoma with 64Cu-SarAr immunoconjugates. *Proc. Natl. Acad. Sci. U. S. A. 104*, 17489−17493.
(48) Wu, Y., Zhang, X., Xiong, Z., Cheng, Z., Fisher, D. R., Liu, S., Gambhir, S. S., and Chen, X. (2005) microPET imaging of glioma integrin alpha(V)beta(3) expression using Cu-64-labeled tetrameric RGD peptide. *J. Nucl. Med. 46*, 1707−1718.
(49) Waibel, R., Alberto, R., Willuda, J., Finnern, R., Schibli, R., Stichelberger, A., Egli, A., Abram, U., Mach, J. P., Plückthun, A., and Schubiger, P. A. (1999) Stable one-step technetium-99m labeling of His-tagged recombinant proteins with a novel Tc(I)-carbonyl complex. *Nat. Biotechnol. 17*, 897−901.
(50) Cai, H., and Conti, P. S. (2013) RGD-based PET tracers for imaging receptor integrin alpha(v)beta(3) expression. *J. Labelled Compd. Radiopharm. 56*, 264−279.
(51) Pandya, D. N., Bhatt, N., Dale, A. V., Young Kim, J., Lee, H., Su, H. Y., Lee, J.-E., Il An, G., and Yoo, J. (2013) New bifunctional chelator for Cu-64-immuno-positron emission tomography. *Bioconjugate Chem. 24*, 1356−1366.
(52) Goethals, P., Volkaert, A., Vandewielle, C., Dierckx, R., and Lameire, N. (2000) 55Co-EDTA for renal imaging using positron emission tomography (PET): a feasibility study. *Nucl. Med. Biol. 27*, 77−81.
(53) Jansen, H. M., Decoo, D., and Minderhoud, J. M. (1997) Co-registration of PET and MRI in different courses of MS using Cobalt-55 as a Calcium-tracer. *Acta Neurol. Belg. 97*, 178−182.
(54) Meredith, R. F., Torgue, J., Azure, M. T., Shen, S., Saddekni, S., Banaga, E., Carlise, R., Bunch, P., Yoder, D., and Alvarez, R. (2014) Pharmacokinetics and imaging of (212)Pb-TCMC-trastuzumab after intraperitoneal administration in ovarian cancer patients. *Cancer Biother. Radiopharm 29*, 12−17.
(55) Nielsen, G. D., Andersen, O., and Jensen, M. (1993) Toxicokinetics of nickel in mice studied with the $\gamma$-emitting isotope nickel-57. *Fundam. Appl. Toxicol. 21*, 236−43.
(56) Zweit, J., Carnochan, P., Goodall, R., and Ott, R. (1994) Nickel-57-doxorubicin, a potential radiotracer for pharmacokinetic studies using PET: production and radiolabelling. *J. Nucl. Biol. Med. 38*, 18−21.
(57) Ciaccio, N. A., Moreno, M. L., Bauer, R. L., and Laurence, J. S. (2008) High-yield expression in E. coli and refolding of the bZIP domain of activating transcription factor 5. *Protein Express. Purif. 62*, 235−243.
(58) Schägger, H. (2006) Tricine-SDS-PAGE. *Nat. Protoc. 1*, 16−22.
(59) Delaglio, F., Grzesiek, S., Vuister, G. W., Zhu, G., Pfeifer, J., and Bax, A. (1995) NMRPipe: a multidimensional spectral processing system based on UNIX pipes. *J. Biomol. NMR 6*, 277−293.
(60) Goddard, T. D., and Kneller, D. G. (2004) *SPARKY*, University of California, San Francisco.
(61) Crapo, J. D., McCord, J. M., and Fridovich, I. (1978) Preparation and assay of superoxide dismutases. *Methods Enzymol. 53*, 382−393.
(62) Tabbi, G., Driessen, W. L., Reedijk, J., Bonomo, R. P., Veldman, N., and Spek, A. L. (1997) High superoxide dismutase activity of a novel, intramolecularly imidazolato-bridged asymmetric dicopper(II) species. Design, synthesis, structure, and magnetism of copper(II) complexes with a mixed pyrazole-imidazole donor set. *Inorg. Chem. 36*, 1168−1175.